A Class of Waveguide Filters for Over-Moded Applications

CHUNG-LI REN AND HAN-CHIU WANG

Abstract—As the frequency spectrum extends to the millimeter wave range, the rapid rise in intrinsic loss and the diminishing physical dimensions greatly curtail the usefulness of conventional waveguide filters in dominant mode waveguide. The incentive for designing filters in over-moded waveguide is all too apparent. However, filter design in over-moded waveguide faces challenging design criteria, such as mode conversion loss and intrinsic loss, ease of being analyzed and synthesized, and feasibility for economical fabrication. A filter structure is presented which fulfills all aspects of the design objectives. The structure involves a type of discontinuity which is not only free from mode conversion but also extremely simple to characterize analytically. The latter renders feasible the use of available filter synthesis techniques. While the proposed filter structure can be designed either as a bandpass filter, a bandstop filter or a low-pass filter in an over-moded uniform waveguide of arbitrary cross section, for illustration purposes only the low-pass filter in over-moded circular waveguide is discussed in great detail. Design theories are presented which allow the proposed structure to be designed either by the image method or by operating parameter filter synthesis. Excellent agreement between the theory and measurements made on filter models is shown.

I. INTRODUCTION

IN a two-way transmission system, the leakage of the high-level transmitter signals into the receiving paths in the channel multiplexing networks can cause serious system degradations. Filters are therefore needed in the multiplexing networks to protect the receiving channels. Since the lower frequency channels are isolated from the higher frequency channels by the cutoff behavior of the waveguides while the reverse is not true, a simple filtering scheme using low-pass filters may be practical.

Numerous known microwave low-pass filter structures are available in the literature [1]. However, these known structures are applicable for dominant mode waveguides only. In a waveguide transmission system [2], every receiving channel would have required one such filter, and a very large number of filters would have been needed in the entire multiplexing system.[1] Furthermore, in the millimeter wave frequency range, the intrinsic loss of these known structures will be prohibitively high, and their diminishing dimensions will be too small to be fabricated economically. An alternative scheme is to place the low-pass filters in the over-moded main signal paths before the channelizing networks, hence only a few broad-band low-pass filters are required. The Marcatili interferometer low-pass filter [3], which has the required broad-band characteristics and steep cutoff response, is useful for such purpose. However, the scope of its application is limited by its low stopband insertion loss (IL) and its relatively high IL in the passband due to mode conversion.

A low-pass filter structure[2] is proposed for this purpose, as shown in Fig. 1, which consists of a parallel array of transverse low-loss dielectric disks in a highly over-moded circular waveguide with the circular electric mode ($H_{01}{}^0$ mode) propagating. The material of each dielectric disk is homogeneous and isotropic so that there can be no mode conversion in the filter structure [5]. Thus the resultant filter has very low intrinsic loss, and its physical dimensions are large for easy fabrication. In addition, because the waveguide is highly oversized for most of the modes concerned in the design, the waveguide can be regarded as nondispersive. The stopband of the filter provides isolation for the $H_{01}{}^0$ mode as well as most of the undesired modes which might exist in the system. The latter is evidently one of the most desirable design criteria for the component design in a highly over-moded region.

The exact design formula is presented for the structure to be designed either as a periodic structure or as a direct-coupled waveguide filter using either the image method or modern filter synthesis, respectively. The image method is preferred, if the desired passband is far away from the cutoff frequency of the stopband. The resultant filter consists of uniformly spaced dielectric disks of identical thickness and, therefore, is economical to fabricate. In the case where the passband is required to be very close to the cutoff frequency of the stopband, the image method may fail. Since the image impedance varies rapidly with frequency near the cutoff frequency of the filter, a broad-band match in the passband will be very difficult to achieve and, therefore, the direct filter synthesis approach should be used. However, the dielectric disks and their spacings will have more variation in thickness for this design as compared to that of the image design. The fabrication cost may, therefore, be higher.

Two low-pass filters are designed using the image method. Each filter has a 30-percent passband bandwidth. To illustrate the application range of the proposed design method, the upper edge of the passband of one filter is 19.5 GHz away from its cutoff frequency of 73.5 GHz, while, for the second filter, it is only 4.5 GHz away from its cutoff frequency of 79 GHz. The measured performance of both filters agrees very well with the theory. The third filter is designed to have a passband from 55–74.7 GHz, and a stopband at 76 GHz. It is designed as a Chebyshev direct-coupled waveguide filter with 21

Manuscript received May 6, 1974; revised August 30, 1974.
The authors are with Bell Laboratories, North Andover, Mass. 01845.

[1] There could be as many as 120 channels.

[2] The authors are grateful to the reviewer for pointing out the known filtering principle of multilayer dielectric stacks reported earlier in the literature [4]. However, the structure requires at least three different dielectric materials with specific dielectric constants. The availability of the appropriate dielectric material and its associated matching problems are viewed as the potential limitation to its applications in practice. For further comparison of the two design approaches and features, the readers are referred to [4].

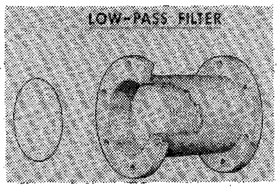

Fig. 1. Dielectric disk low-pass filter.

cavities (22 dielectric disks). Excellent agreement between theory and measurements has also been established. The passband IL of all three filters is measured to be less than 0.1 dB which indicates that the intrinsic loss as well as the mode conversion level in the filter structure are extremely low, as expected. The measured cutoff frequency of the low-pass filter has been shown to fluctuate less than 0.1 GHz over the temperature range of 53–96°F.

Although tight tolerance is required on disk thickness and spacing, it has been proven to be practical and economical to produce filters by conventional machining processes because of their simple geometry. Close agreement between the measured performance and the theory can be assured with reasonable mechanical tolerances without the necessity of any individual cavity tuning. For operation in an over-moded waveguide region, it is very desirable to avoid any tuning device which may often cause moding problems and complicate the mechanical design.

II. DESIGN PRINCIPLES

In the design of the waveguide components, accurate theoretical design information is often lacking because the components generally involve complicated coupling structures and waveguide discontinuities. Measured data rather than the approximated electromagnetic (EM) field solutions are usually the foundation of a successful design. However, in a highly over-moded region, obtaining reliable measured data is a very difficult if not impossible task indeed (for example, several hundreds of modes for frequencies in the millimeter wave range can propagate in a 2-in-diameter circular waveguide). In contrast, the "discontinuities" involved in the proposed structure are merely a cascade of dielectric interfaces which, in terms of EM field solutions, can be characterized exactly as a cascade of transmission lines. The theoretical treatment to be presented in this paper will therefore be exact.

A. The Image Method—Design of the Dielectric Disk Filter as a Periodic Structure

The design of the proposed filter on the image parameter basis consists of two steps. First, a filter section is designed as a periodic structure consisting of identical dielectric disks with equal spacings between the disks. To ensure good return loss in the passband, a matching network with varying disk thickness and spacing is added to both sides of the filter section.

1) Design Formula for Filter Section (Periodic Structure): The unit cell of the periodic filter section is shown in Fig. 2. The image impedance Z_I and the equivalent electrical length of the unit cell $\hat{\theta}$ are given by

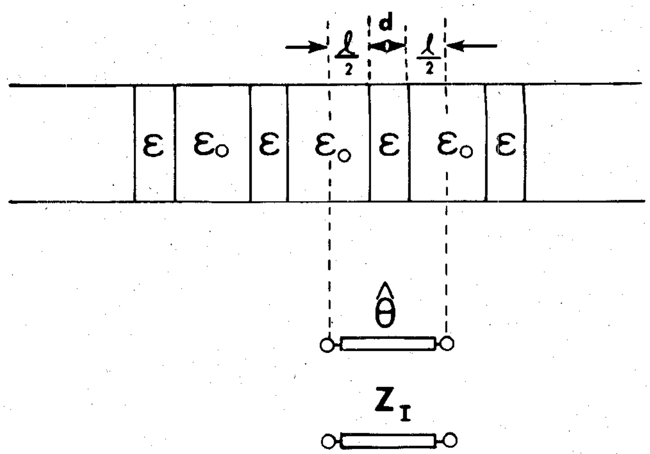

Fig. 2. Periodic structure—filter section.

$$Z_I = Z_0\left(\frac{1+\frac{1}{2}\tan\theta_\epsilon(Z_\epsilon/Z_0\cot\theta - Z_0/Z_\epsilon\tan\theta)}{1-\frac{1}{2}\tan\theta_\epsilon(Z_\epsilon/Z_0\tan\theta - Z_0/Z_\epsilon\cot\theta)}\right)^{1/2} \quad (1)$$

$$\hat{\theta} = \cos^{-1}\left[\cos\theta_\epsilon\cos 2\theta - \tfrac{1}{2}(Z_\epsilon/Z_0 + Z_0/Z_\epsilon)\cdot\sin\theta_\epsilon\sin 2\theta\right] \quad (2)$$

$$\theta_\epsilon = \beta_\epsilon d \qquad \theta = \tfrac{1}{2}\beta l.$$

Z_0 and Z_ϵ are the characteristic impedances of the specific mode in the empty waveguide and dielectric waveguide, respectively. β and β_ϵ are the propagation constants corresponding to Z_0 and Z_ϵ. Z_I and $\hat{\theta}$ exhibit alternating passbands and stopbands which is characteristic for a periodic structure as shown in Fig. 3.

Let f_c^l and f_c^h be the lower and upper edges of each stopband, respectively. It can be easily seen from (1)

$$[\tan\beta\tfrac{1}{2}l]_{f_c^l} = [Z_\epsilon/Z_0\cot\beta_\epsilon\tfrac{1}{2}d]_{f_c^l} \quad (3)$$

and

$$[\tan\beta\tfrac{1}{2}l]_{f_c^h} = [Z_0/Z_\epsilon\cot\beta_\epsilon\tfrac{1}{2}d]_{f_c^h}. \quad (4)$$

ϵ is the relative dielectric constant of the dielectric disks in the filter. When f_c^l and f_c^h are given (the design objectives), the solution l and d for a specific value ϵ may be obtained by solving (3) and (4). To gain some insight from (3) and (4), a simplification is made for designs involving highly over-moded waveguides. Since the waveguide is highly over-moded, the propagation constant β and β_ϵ can be approximated as nondispersive, i.e., $\beta \simeq k$, $\beta_\epsilon \simeq (k\epsilon)^{1/2}$, and $k = 2\pi(\mu\epsilon_0)^{1/2}f$. Under this assumption, (3) and (4) can be written

$$\tan\left(\frac{\pi l}{c}f_c^l\right) \simeq \epsilon^{-1/2}\cot\left(\frac{\pi d\epsilon^{1/2}}{c}f_c^l\right) \quad (5)$$

$$\tan\left(\frac{\pi l}{c}f_c^h\right) \simeq \epsilon^{1/2}\cot\left(\frac{\pi d\epsilon^{1/2}}{c}f_c^h\right), \qquad c = (\mu\epsilon_0)^{-1/2}. \quad (6)$$

Equation (6) can be also written as

$$\tan\left(\frac{\pi}{2} - \frac{\pi d\epsilon^{1/2}}{c}f_c^h\right) \simeq \epsilon^{-1/2}\cot\left(\frac{\pi}{2} - \frac{\pi l}{c}f_c^h\right). \quad (7)$$

From (5) and (7), we get

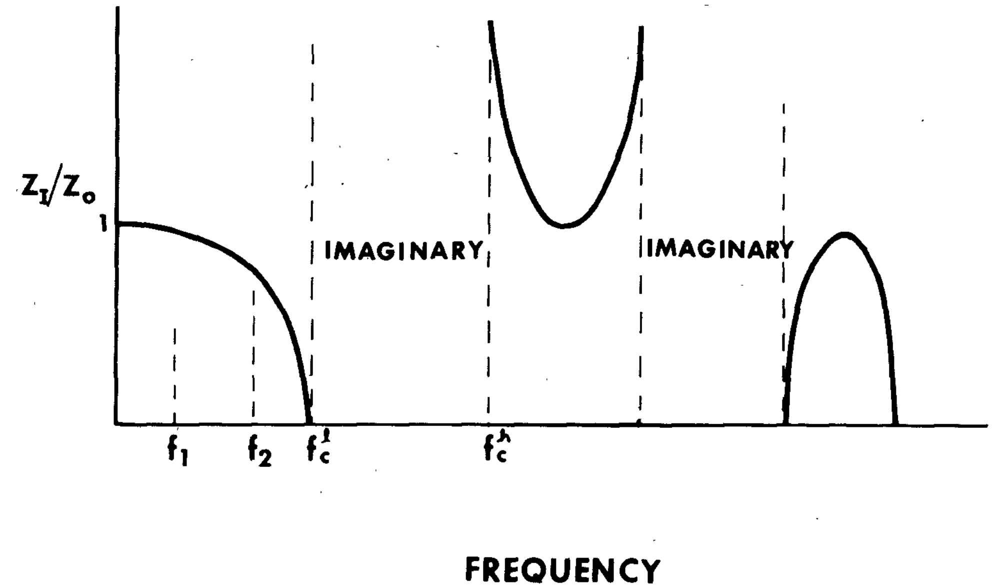

Fig. 3. Image impedance.

$$d = \frac{l}{\epsilon^{1/2}}. \tag{8}$$

From (5), (6), and (8) we get

$$l = \frac{c}{\pi f_c^{\,l}} \tan^{-1} (\epsilon^{-1/4}) \tag{9}$$

and

$$\epsilon \geq \tan^4 \left[\frac{\pi}{2} \frac{f_c^{\,h}}{f_c^{\,l} + f_c^{\,h}} \right]. \tag{10}$$

Equation (10) is plotted in Fig. 4. The plots in Fig. 4 can be used to determine the required dielectric constant for a stopband with specified bandwidth. It might be pointed out that, in practice, the designer must also take into account other design factors along with the bandwidth considerations. The dielectric material should have low loss, mechanical strength, and machinability. It is also preferred to choose the lowest possible ϵ to fulfill the bandwidth requirement and, at the same time, to have reasonable physical thickness of the dielectric disks in the design. After ϵ is determined, d and l of the unit cell can be computed from (8) and (9), respectively.

In the case where the waveguide is not over-moded and the mode concerned in the design becomes highly dispersive, similar design equations should be derived directly from (3) and (4).

The number of the dielectric disks of the periodic filter section can be determined from the IL of each unit cell:

$$\mathrm{IL} = (20 \log e) \{ \cosh^{-1} [\tfrac{1}{2}(Z_\epsilon/Z_0 + Z_0/Z_\epsilon) \sin \theta_\epsilon \sin 2\theta - \cos \theta_\epsilon \cos 2\theta] \} \text{ dB}. \tag{11}$$

2) Design Formula for Matching Networks: A matching network is required at both ports of the periodic filter section to match the image impedance of the periodic structure Z_I into the characteristic impedance of the waveguide. Depending upon the bandwidth in which the

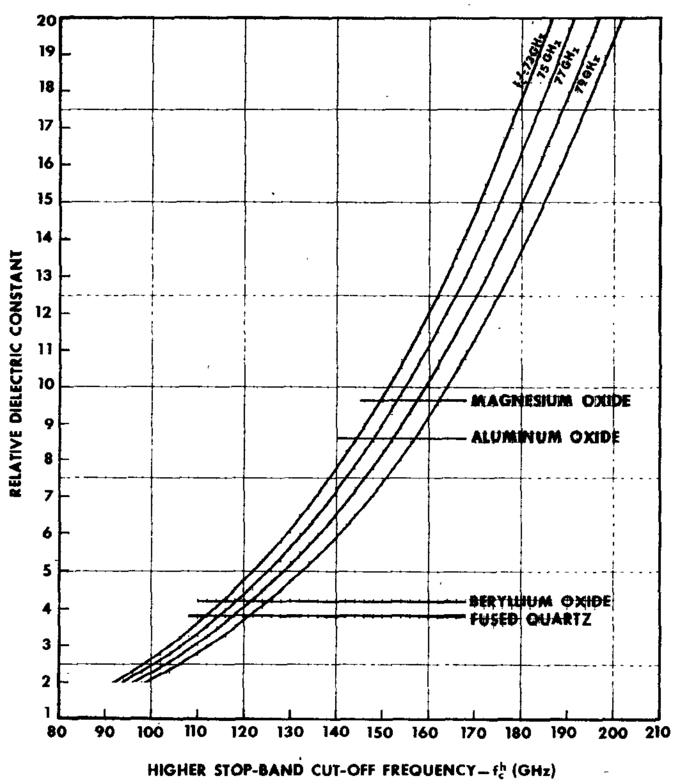

Fig. 4. Relative dielectric constant versus cutoff frequency.

impedance of the periodic filter structure is to be matched, one or more matching dielectric disks may be required for the matching networks.

For the case where the passband (f_1–f_2 as shown in Fig. 3) is not too close to cutoff frequency, a simple design technique of the matching network is shown to be practical. Since the filter characteristic impedance Z_I is not varying much with frequency, the matching network may be designed as an impedance transformer [1] between $Z_I(f_0)$ and Z_0, Fig. 5. f_0 is the center of the passband.

Once the number of sections is chosen, the characteristic

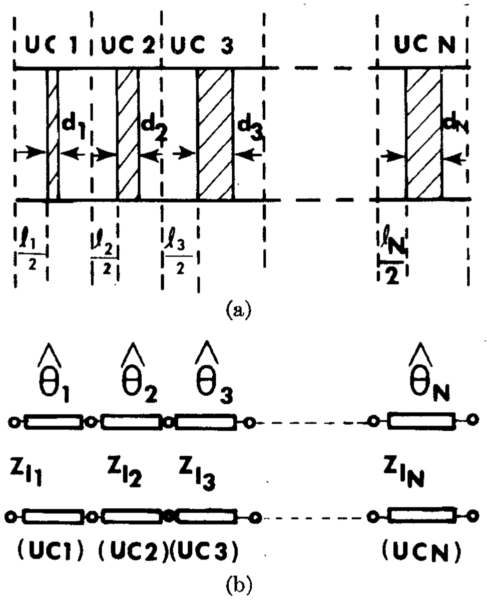

Fig. 5. The matching networks.

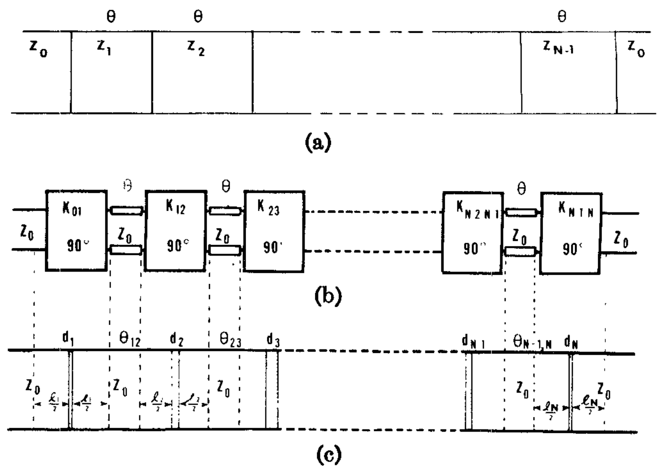

Fig. 6. Synthesis of the disk-loaded waveguide as direct-coupled waveguide filters. K_{ij}—characteristic impedance of inverter; d_i—thickness of dielectric disk; θ_{ij}—electrical length between the dielectric disks; Z_0—characteristic impedance of circular waveguide; θ—identical electrical length between the inverters; Z_i—stepped impedance.

TABLE I

n	m_1	m_2	m_3	m_4
2	$\frac{1}{4}$	$\frac{3}{4}$	--	--
3	$\frac{1}{8}$	$\frac{1}{2}$	$\frac{7}{8}$	--
4	$\frac{1}{16}$	$\frac{5}{16}$	$\frac{11}{16}$	$\frac{15}{16}$

Note: n—number of sections; $Z_{Ii}/Z_0 = (Z_I/Z_0)m_i$.

impedance of ith matching section Z_{Ii} can be either obtained from design tables [1] or Table I. Table I gives the approximated values of Z_{Ii}/Z_0 which become quite accurate for the range of Z_I/Z_0 encountered in the image design and is convenient to use. For example, $n = 4$ and $Z_I/Z_0 = 0.5$, Z_{Ii} computed from Table I are off by only 0.016 percent from their exact values.

The physical dimension of the ith air spacing l_i and its associated matching dielectric disk d_i can be computed from (1) and (2) at $f = f_0$,

$$l_i = \frac{2}{\beta}\tan^{-1}\left(\frac{1-(Z_{Ii}/Z_\epsilon)^2}{(Z_{Ii}/Z_0)^2-(Z_0/Z_\epsilon)^2}\right)^{1/2} \qquad (12)$$

and

$$d_i = \frac{1}{\beta_\epsilon}\tan^{-1}\left(\frac{2}{Z_\epsilon/Z_0+Z_0/Z_\epsilon}\cot\beta l_i\right). \qquad (13)$$

B. The Synthesis Method

A uniform waveguide loaded with transverse dielectric disks [Fig. 6(c)] can be designed as a direct-coupled waveguide filter [Fig. 6(b)] using the filter synthesis approach.

The impedance inverters of the prototype direct-coupled waveguide filter shown in Fig. 6(b) are equivalent to their corresponding dielectric disks in the waveguide with a length of waveguide on either side of the dielectric disk [Fig. 6(c)]. The equivalence is defined at a reference frequency. In the design of a low-pass filter, the cutoff frequency is generally used as the reference frequency [6]. θ is equal to 180° at this reference frequency throughout Fig. 6. Once the characteristic impedance K of the impedance inverter is given, the thickness of the dielectric disk d and the length of the waveguide on both sides of the dielectric disk $l/2$ can be derived from (1) and (2) by letting $\hat{\theta} = (\pi/2)$.

$$d = \frac{1}{\beta_\epsilon}\sin^{-1}\left(\frac{Z_0/K - K/Z_0}{Z_0/Z_\epsilon - Z_\epsilon/Z_0}\right) \qquad (14)$$

and

$$l = \frac{1}{\beta}\cot^{-1}\left[\frac{1}{2}\left(\frac{Z_0}{Z_\epsilon}+\frac{Z_\epsilon}{Z_0}\right)\tan(\beta_\epsilon d)\right]. \qquad (15)$$

Equations (14) and (15) are identical to the results of the coaxial disk capacitor structure treated by David and Khan [7] and by Levy [6]. It is important to point out that ϵ is implicitly constrained by (14). Noting that $|\sin(\beta_\epsilon d)| \leq 1$ in (14), we get

$$\left|\frac{Z_0/K - K/Z_0}{Z_0/Z_\epsilon - Z_\epsilon/Z_0}\right| \leq 1. \qquad (16)$$

For a given value of K, there exists a minimum value of dielectric constant in (16), for which a set of solutions for d and l can be found from (14) and (15).

A step-by-step design procedure for the dielectric-disk waveguide structure is outlined as follows.

1) A stepped-impedance half-wave filter as shown in Fig. 6(a) with the desired characteristics is chosen according to the design objectives. The characteristic impedances Z_i may be found readily from the design tables in [8].

2) The inverter impedances $K_{i,i+1}/Z_0$ in Fig. 6(b) are obtainable from the Z_i in Fig. 6(a) by establishing the

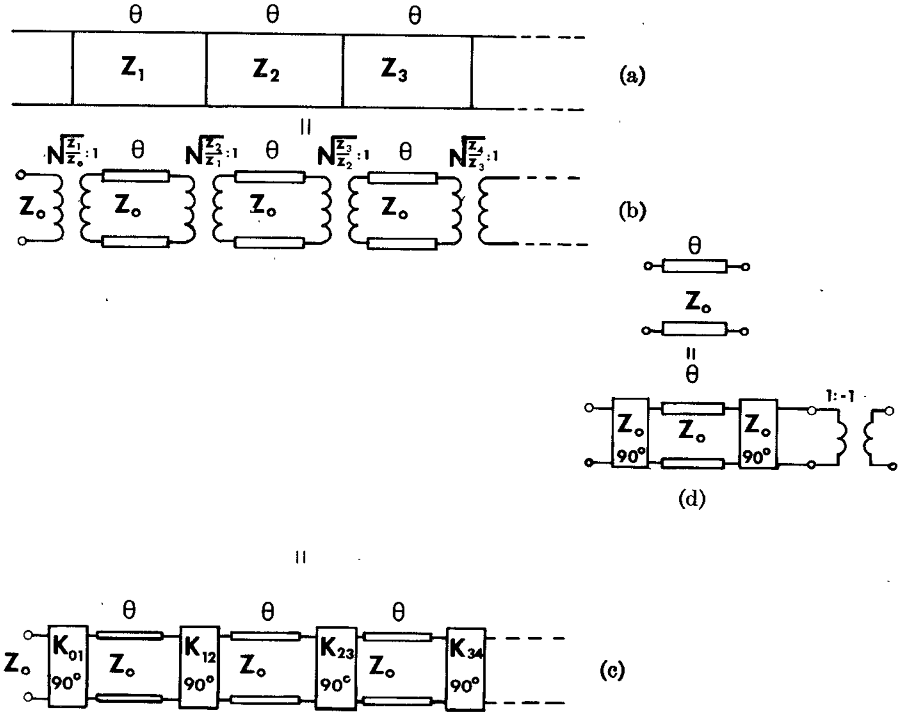

Fig. 7. Network transformations.

equivalence between these two circuits as shown in Fig. 7. Fig. 7(a) can be represented as in Fig. 7(b) with all transmission lines normalized to Z_0. To insert inverters between all adjacent half-wave transmission lines as in Fig. 7(c), the network transformation of Fig. 7(d) is applied to each and every nonadjacent half-wave line in Fig. 7(b). Depending upon whether the transformation is starting from the first or the second half-wave line from the input port, all $K_{i,i+1}/Z_0$ will either be greater than unity or less than unity, respectively. Noting from (14) that, for $K_{i,i+1}/Z_0 < 1$, $\beta_\epsilon d$ will be in the first or second quadrant and, for $K_{i,i+1}/Z_0 > 1$, $\beta_\epsilon d$ will be in the third or fourth quadrant, the solution of $K_{i,i+1}/Z_0 < 1$ is preferred for smaller d to achieve broader bandwidth. We then have

$$K_{i,i+1}/Z_0 = \begin{cases} (Z_i/Z_{i+1})^{1/2} \text{ at the step where } Z_{i+1} > Z_i \\ (Z_{i+1}/Z_i)^{1/2} \text{ at the step where } Z_{i+1} < Z_i. \end{cases} \tag{17}$$

3) $K_{i,i+1}/Z_0$ as computed from (17) is monotonically decreasing from the input port toward the center of the filter. Therefore, the center inverter has the minimum value of $K_{i,i+1}/Z_0$. If the same dielectric material shall be used for all dielectric disks in the filter, the minimum dielectric constant of this dielectric material must be determined from (16) using the minimum value of $K_{i,i+1}/Z_0$ in the filter synthesis.

4) With all $K_{i,i+1}/Z_0$ computed from (17), their corresponding d_i and l_i can be computed from (14) and (15) at the reference frequency. For obtaining broad-band characteristics, the solution of $\beta_\epsilon d_i$ and βl_i in (14) and (15) should both be in the first quadrant. The total waveguide length between the ith and $(i+1)$th disk is given by

$$L_{i,i+1} = \tfrac{1}{2}l_i + \tfrac{1}{2}l_{i+1} + \pi/\beta_c \tag{18}$$

where β_c is the propagation constant in the waveguide at f_c^l.

III. DESIGN EXAMPLES

Three dielectric-disk low-pass filters have been designed and fabricated. Two filters were designed using the image method and the third filter was synthesized as a 21-cavity Chebyshev low-pass filter.

A. Design Examples—The Image Method

1) Design Example 1: Passband: $f_1 = 40$ GHz, $f_2 = 54$ GHz. VSWR ≤ 1.05 in the passband; IL between 76 GHz and 110 GHz ≥ 80 dB.

It is determined from Fig. 4 that the fused quartz disks with a dielectric constant of 3.78 [9] will provide a stopband with $f_c^l = 73.5$ GHz and $f_c^h = 112$ GHz. From (11), it is found that a 30-disk periodic structure will be sufficient to provide greater than 80-dB IL for frequencies ranging from 76–110 GHz.

The matching networks are based on the design principle of the quarter-wave transformer as described in Section II. Since the passband is relatively far away from the stopband in the design specification, the image impedance is relatively flat in the passband. The center of the passband at $f_0 = 47$ GHz is chosen as the reference frequency. The computed responses of matching networks,

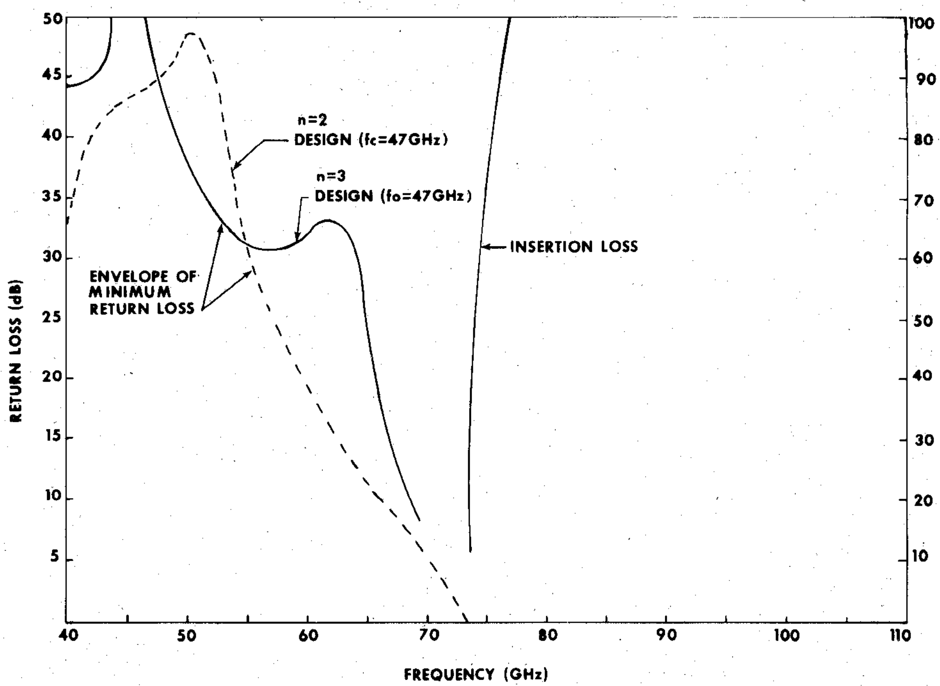

Fig. 8. Theoretical performance of the low-pass filters by image method.

one with two dielectric disks ($n = 2$), and one with three dielectric disks ($n = 3$), are shown in Fig. 8. The $n = 2$ design provides 30-percent passband bandwidth and the $n = 3$ design provides 40-percent passband bandwidth with the return loss greater than 30 dB (VSWR ≤ 1.05).

The thickness of the first dielectric disk is less than 0.003 in which is considered to be too thin to be practical in the fabrication. It is increased to 0.005 in by computer optimization with the minimum return loss slightly degraded in the passband. $n = 3$ is used in this design example.

The photograph of the fabricated filter is shown in Fig. 9. Both the measured passband return loss and the stopband IL are shown in Fig. 10 in good agreement with the theory. (The computed minimum return loss using the measured dimensions of the fabricated filter is shown by the shaded curves in Fig. 10.) The IL in the passband is measured to be less than 0.1 dB. Since the computed theoretical IL is 0.05 dB, the measured IL indicates not only that the intrinsic loss of this filter is indeed very small, but that the mode conversion level is also extremely low. The high IL in the stopband is measured on a point-by-point basis. The cutoff frequency of the low-pass filter has been shown to fluctuate less than 0.1 GHz over the temperature variations of 53–96°F.

2) Design Example 2: Passband: $f_1 = 55$ GHz, $f_2 = 74.5$ GHz; VSWR ≤ 1.05 in the passband; IL between 82 and 110 GHz ≥ 35 dB.

For the specified design objectives, it is determined according to the design steps elaborated in Section II that ten fused quartz disks are required for the periodic filter section with a cutoff frequency of 79 GHz.

In contrast to the first design example, the passband in this design is, in comparison, close to the stopband. The slope of the image impedance of the filter section becomes very steep in the frequency range of the desired passband.

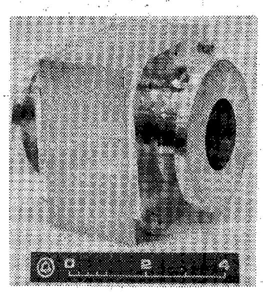

Fig. 9. Photograph of a low-pass filter.

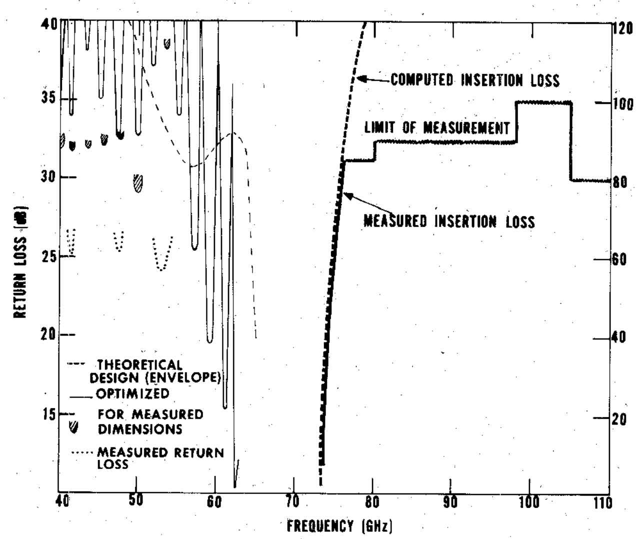

Fig. 10. Computed and measured performance of design example 1.

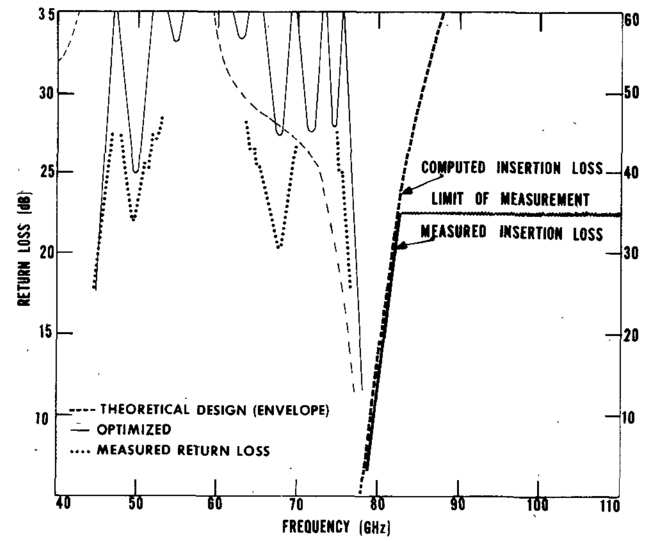

Fig. 11. Computed and measured performance of design example 2.

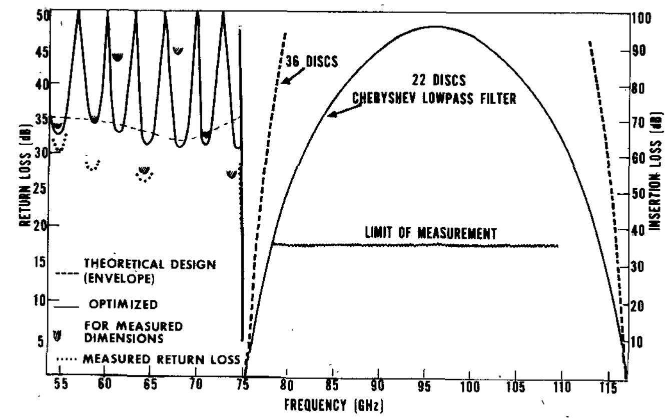

Fig. 12. Computed and measured performance of Chebyshev low-pass filter.

In order to achieve sufficient bandwidth for the matching networks, the reference frequency f_0 can no longer be placed at the center of the passband as in the first design example. For broad-band match, f_0 is usually placed in the vicinity where the image impedance of the filter section is slowly varying. For the second design example, with f_0 being properly placed, a good match can still be obtained for the desired passband. For $f_0 = 51.5$ GHz, the computed return loss of a matching network with three dielectric disks is shown in Fig. 11. In this design, the first disk has a thickness of only 0.0016 in. A computer program is used to optimize the physical parameters of the matching networks based on the parameters of the ideal design. The thickness of the first disk is increased to 0.006 in, with only small degradation in the minimum return loss in the passband, Fig. 11.

The measured performance of the fabricated filter is shown in Fig. 11 in close agreement with the theoretical performance. The IL in the passband is also measured to be less than 0.1 dB.

B. Design Example—The Synthesis Method

Passband: $f_1 = 55$ GHz, $f_2 = 74.7$ GHz; VSWR ≤ 1.05 in the passband; stopband: 76–110 GHz.

With the specified design objectives, it is determined from the design steps described in Section II that 22 fused quartz disks are required in the design of a Chebyshev filter. The computed performance of this filter is shown in Fig. 12. Since the filter is symmetrical, the 22 quartz disks in the filter have eleven different thicknesses ranging from less than 0.002 in for the first disk up to greater than 0.015 in. The thickness of the first thin disk is increased to 0.005 in with the aid of a computer resulting in only a slight degradation of the minimum return loss in the passband, Fig. 12. Since only the first few sections near the input ports are allowed to vary in the process of obtaining a "thick" first disk, the computed stopband characteristics show practically no change as compared to the original design, Fig. 12. The measured performance of the fabricated filter is shown in excellent agreement with the theory, Fig. 12.

It might be pointed out that in the case where a steeper rise of the IL is required in the stopband near the cutoff frequency, additional sections identical to the center section of the 22-disks design may be added without appreciably affecting the passband return loss. A typical example is a filter of 36 quartz disks derived from the 22-disks design by simply adding 14 uniform sections. Its computed performance is compared to that of the 22-disks design in Fig. 12. The 36 quartz disks design can provide greater than 20-dB IL at 76 GHz.

IV. CONCLUSION

As frequencies extend into the millimeter wave region, the trend of filtering in over-moded waveguides can be observed, in order to keep the intrinsic loss low and the physical dimension realistically large. For such an over-moded application, a class of filters using dielectric disks is proposed. In addition to desirable features such as low mode conversion loss, low intrinsic loss, and large dimensions, the proposed structure exhibits two special properties which make it particularly practical. Electrically, this structure can be analytically treated in a rigorous fashion which is not true for most structures in over-moded waveguide. Consequently, numerous known theories and available computer-aided design techniques can readily be applied. Mechanically, because of its simple geometry, tight tolerances can be obtained rather economically though a conventional machining process.

Three broad-band low-pass filters involving over twenty or thirty direct-coupled cavities (formed by the dielectric disks and the waveguide spacings) have been designed in 2-in-diameter circular waveguide. The fabricated filters do not require individual cavity tuning and the expected filter performance is ensured entirely by the exact design theory with a set of obtainable tolerances (± 0.0001 in for the thickness of the disks and their spacings). The measured performance of all three design examples has been shown to be in close agreement with the theory. The measured IL in the passbands are less than 0.1 dB, indicating that the intrinsic losses as well as the mode conversion levels are indeed very low.

Although these filters have been designed as low-pass filters, the close agreement between measurement and analysis strengthens our belief that their application should not be limited in this way. We envision possible applications as broad-band bandpass as well as bandstop filters, in the millimeter wave region as well as in other frequency ranges.

ACKNOWLEDGMENT

The authors wish to thank many of their colleagues at the Bell Laboratories, whose cooperation has made the progress of this project possible. Especially, they would like to thank R. P. Hecken, H. A. Kvinlaug, and J. C. Williams for their efforts in the computer-aided design and physical realization studies during the early phase of this program.

REFERENCES

[1] G. L. Matthaei, L. Young, and E. M. T. Jones, *Microwave Filters, Impedance-Matching Networks and Coupling Structures.* New York: McGraw-Hill, 1964.
[2] P. T. Hutchinson, "A digital millimeter wave waveguide transmission system," in *Trunk Telecommunication by Guided Waves Conference Dig., Publ. No. 71*, 1970, pp. 159–164.
[3] E. A. Marcatili and D. L. Bisbee, "Band splitting filters," *Bell Syst. Tech. J.*, vol. 40, pp. 197–213, Jan. 1961.
[4] L. Young and E. G. Cristal, "Low-pass and high-pass filters consisting of multilayer dielectric stacks," *IEEE Trans. Microwave Theory Tech.*, vol. MTT-14, pp. 75–80, Feb. 1966.
[5] L. B. Felsen and N. Marcuvitz, *Radiation and Scattering of Waves.* Englewood Cliffs, N. J.: Prentice-Hall, 1973.
[6] R. Levy, "A generalized design technique for practical distributed reciprocal ladder networks," *IEEE Trans. Microwave Theory Tech.*, vol. MTT-21, pp. 519–526, Aug. 1973.
[7] W. A. Davis and P. J. Khan, "Coaxial bandpass filter design," *IEEE Trans. Microwave Theory Tech.*, vol. MTT-19, pp. 373–380, Apr. 1971.
[8] R. Levy, "Tables of element values for the distributed low-pass prototype filter," *IEEE Trans. Microwave Theory Tech.* (*Special Issue on Microwave Filters*), vol. MTT-13, pp. 514–536, Sept. 1965.
[9] *Dielectric Materials and Applications*, A. R. Von Hippel, Ed. Cambridge, Mass.: M.I.T. Press, 1954.

Integrated Fin-Line Millimeter Components

PAUL J. MEIER, SENIOR MEMBER, IEEE

Abstract—**This paper reviews the characteristics of integrated fin-line, a low-loss transmission line which is compatible with batch-processing techniques and superior to microstrip in several respects at millimeter wavelengths. Relative to microstrip, fin-line can provide less stringent tolerances, greater freedom from radiation and higher mode propagation, better compatibility with hybrid devices, and simpler interfaces with waveguide instrumentation. Examples of solid-state and passive components are presented which illustrate the potential of integrated fin-line at millimeter wavelengths. The examples include a p-i-n attenuator which has demonstrated the capability of constructing low-loss semiconductor mounts in fin-line. A four-pole bandpass filter, which performs in close agreement with theory, is also discussed.**

INTRODUCTION

INCREASED activity in the spectrum above 30 GHz has recently stirred interest in the development of millimeter integrated circuits. Much of the enthusiasm associated with integrated circuits can be traced to the clear advantages that such circuits provide below 3 GHz, namely, reduced size, weight, and cost combined with improved electrical performance, production uniformity, and reliability. However, those who have worked with integrated circuits at centimeter wavelengths (3–30 GHz) have encountered some fundamental problems which have limited the utility of such circuits. These problems include the critical tolerances and questionable production uniformity that can occur when miniaturization is carried too far. Although enhanced performance is possible in centimeter integrated circuits through the reduction of parasitics and the elimination of superfluous interfaces, poorer overall performance is also possible. The fundamental microstrip problems, which generally increase in severity as the operating frequency is raised, include radiation loss, spurious coupling, dispersion, and higher mode propagation. Attempts to integrate a large number of components in a single housing have generally demonstrated the need for "mode barriers" and "box-resonance absorbers." Radiation and related problems can be controlled by choosing progressively thinner substrates as the operating frequency is raised, but this only serves to degrade the Q factor, compound tolerance problems, and restrict the range over which the characteristic impedance can be varied.

Although standard microstrip techniques can be applied to millimeter components [1], [2], the problems listed

Manuscript received May 8, 1974; revised August 30, 1974.
The author is with AIL, a Division of Cutler-Hammer, Melville, N. Y. 11746.